Hindawi Publishing Corporation
Advances in Materials Science and Engineering
Volume 2015, Article ID 734396, 5 pages
http://dx.doi.org/10.1155/2015/734396

Research Article

Structural and X-Ray Photoelectron Spectroscopy Study of Al-Doped Zinc-Oxide Thin Films

Bong Ju Lee,[1] Ho Jun Song,[2] and Jin Jeong[1]

[1]*Department of Physics, Chosun University, Gwangju 501-759, Republic of Korea*
[2]*Department of Dental Materials, School of Dentistry, Chonnam National University, Gwangju 500-757, Republic of Korea*

Correspondence should be addressed to Jin Jeong; jeji@chosun.ac.kr

Received 5 January 2015; Accepted 4 March 2015

Academic Editor: You Song

Al-doped zinc-oxide (AZO) thin films were prepared by RF magnetron sputtering at different oxygen partial pressures and substrate temperatures. The charge-carrier concentrations in the films decreased from 1.69×10^{21} to 6.16×10^{17} cm^{-3} with increased gas flow rate from 7 to 21 sccm. The X-ray diffraction (XRD) patterns show that the (002)/(103) peak-intensity ratio decreased as the gas flow rate increased, which was related to the increase of AZO thin film disorder. X-ray photoelectron spectra (XPS) of the O1s were decomposed into metal oxide component (peak A) and the adsorbed molecular oxygen on thin films (peak B). The area ratio of XPS peaks (A/B) was clearly related to the stoichiometry of AZO films; that is, the higher value of A/B showed the higher stoichiometric properties.

1. Introduction

Aluminum-doped zinc-oxide (AZO) films have been intensively investigated in recent years because their electrical properties make them suitable for a wide range of applications [1–5]. A number of different methods are currently used to fabricate AZO thin films, the most common being magnetron sputtering [6, 7], pulsed laser deposition [8], chemical vapor deposition [9], chemical spray deposition [10], pulsed laser deposition (PLD) [11], and atomic layer deposition (ALD) [12–16]. Magnetron reactive sputtering with a Zn-Al alloy target provides advantages related to target fabrication and film deposition rate [17]. However, a drawback of this method is that the chemical composition of the deposited AZO thin films changes as the Zn at the substrate surface oxidizes, a reaction that is difficult to control. The other conventional physical deposition techniques generally produce good-quality transparent films, though they are very expensive and difficult to apply at industrial scales.

The electronic properties of AZO thin films are closely related to the structural defects at their surface. In our previous report [18], we measured the carrier density as a function of the substrate temperature. However, there have been few studies on the structural, Hall-effect, and X-ray photoelectron spectroscopy (XPS) characteristics of AZO thin films deposited on Si substrates. In this paper, we present the results of a study of the structural and electrical properties of AZO films deposited on a Si substrate at different oxygen partial pressures and various substrate temperatures. We report the X-ray diffraction (XRD) patterns, Hall-effect data, and XPS characteristics of the AZO thin films.

2. Experiment

AZO thin films were deposited on Si (001) surfaces using radio frequency (RF) magnetron sputtering. An AZO ceramic specimen (5N purity, Cerac Inc.,) containing 2 wt.% Al_2O_3 was used as the sputtering target. The chamber was first reduced to a vacuum pressure of $<5 \times 10^{-5}$ Pa and then filled with a mixture of N_2 and O_2 through independent mass-flow controllers to the specified oxygen partial pressure. The RF deposition temperatures used were 350 and 450°C, and the Al target power was 90 W throughout the experiment. The target substrate distance was fixed at 2.5 cm, as was the deposition time at 3 hours. The various film sample designations and processing parameters are listed in Table 1.

The crystallinity and epitaxial growth of the AZO films were investigated using XRD (Rix-2000, Rigaku, Japan). The

Table 1: Deposition conditions for the Al-doped ZnO thin film samples.

Sample	Deposition time (hr)	Deposition temperature (°C)	Gas flow rate N : O (sccm)	Power (W)
A450-7	3	450	7 : 7	90
A350-7	3	350	7 : 7	90
A350-14	3	350	14 : 14	90
A350-21	3	350	21 : 21	90

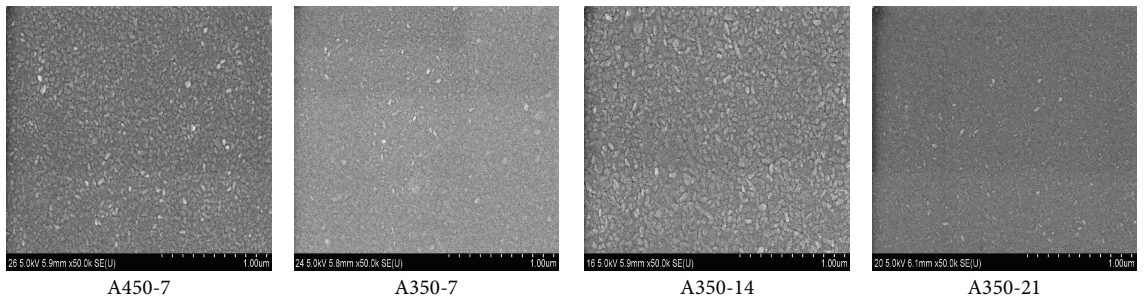

(a)

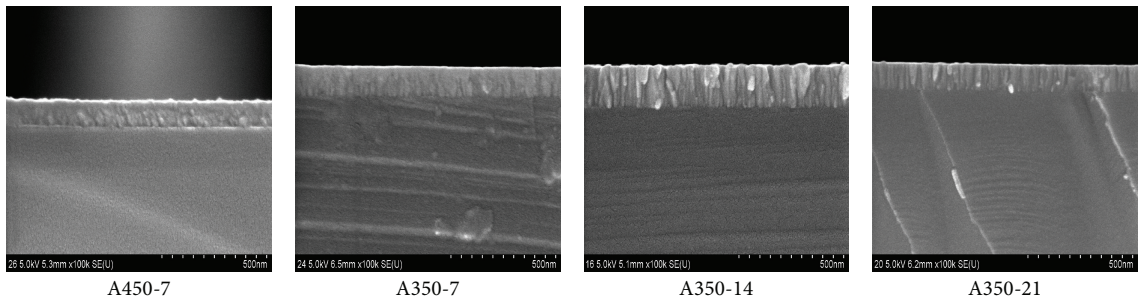

(b)

Figure 1: SEM images of (a) the surfaces and (b) the cross sections of the AZO thin films.

surface morphology and thickness of the films were evaluated by using scanning electron microscopy (SEM, Hitachi S-4200). The electrical properties of the AZO films were inquired into by using the Hall measurements by the van der Pauw method. The stoichiometry of the ZnO thin films was confirmed by X-ray photoelectron spectrometer (Kratos AXIS-HS) with a monochromatized Mg Kα X-ray source.

3. Results and Discussion

Figure 1 shows SEM images of the surfaces and cross sections of the AZO films. As shown in the topographic images in Figure 1(a), the grain sizes of the A450-7, A350-7, A350-14, and A350-21 samples were 0.1, 0.1, 0.07, and 0.05 μm, respectively. The grain size decreased as the gas flow rate increased for A350-7, A350-14, and A350-21 in a row. However, at the substrate temperature of 450°C, the grain size of the thin films did not change. Figure 1(b) shows cross-sectional SEM images of the AZO films. At higher gas flow rates, the cross sections clearly indicate strongly oriented crystallites perpendicular to the substrate. Crystallite sizes insignificantly changed with substrate temperature. However, the crystallite sizes decreased significantly with increased gas flow rate. It is apparent from the images in Figure 1(b) that the AZO film thickness changed a little; it was 0.11, 0.12, 0.20, and 0.11 μm (from left to right). The thickness of AZO film increased a little, as temperature decreased from 450 to 350°C. At the same temperature conditions, the thin films thickness increased as gas flow rate increased from 7 to 14 sccm. However, with more increase in gas flow rate to 21 sccm, the film thickness decreased again. It was inferred that the crystal size and thickness of the thin film were affected more by gas flow rate than substrate temperature.

Figure 2 shows the XRD patterns of the Al-doped films, which were determined to have the (polycrystalline) hexagonal wurtzite structure associated with zinc-oxide. The (002)/(103) peak-intensity ratios ($I_{(002)/(103)}$) were 1.03, 0.63, 0.43, and 0.13 for A450-7, A350-7, A350-14, and A350-21, respectively. The value of $I_{(002)/(103)}$ decreased as temperature and oxygen flow rate decrease. The highest $I_{(002)/(103)}$ value of A450-7 thin films shows higher tendency to c-axis direction orientation. With smaller value of I, the thin film tends more to become disordered. The results of XRD analysis showed that the crystal growth direction from the surface became disordered as the substrate temperature decreased

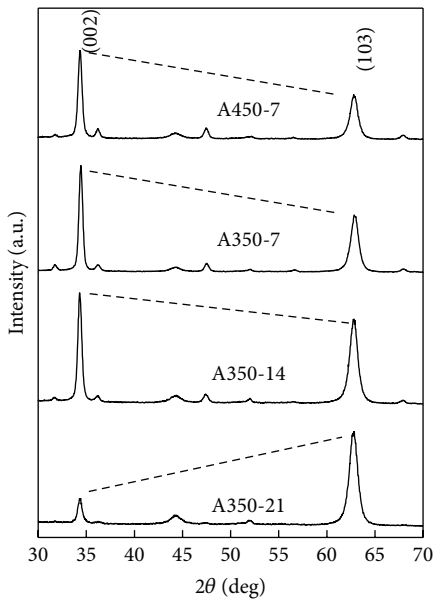

FIGURE 2: XRD patterns of the different AZO films.

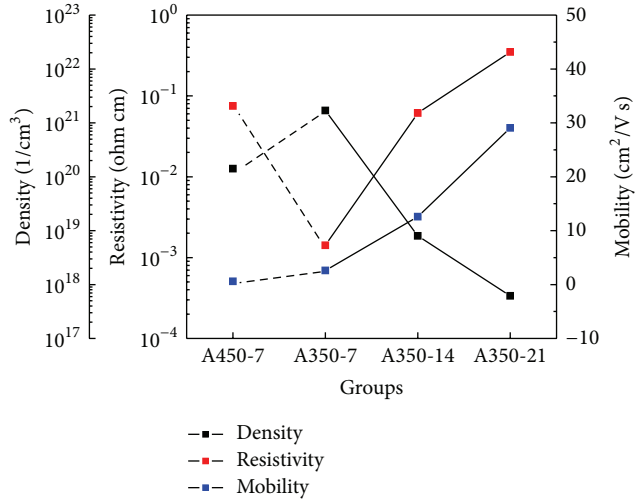

FIGURE 3: Hall-effect data of the AZO films.

and gas flow rate increased. The more disordered the thin films become, the more rough the surface gets. For electrical device applications, ZnO thin films require a small grain size and a high surface-to-volume ratio for enhanced reliability and electrical properties. Such variations in diffraction peak intensities have been reported earlier in the case of Zr-doped ZnO films prepared using the sol-gel method and Ga-doped ZnO films prepared using spray pyrolysis [17, 19].

The 2θ positions of the (002) peaks of A450-7, A350-7, A350-14, and A350-21 were 34.40, 34.47, 34.29, and 34.45°, respectively. In addition to the c-axis orientation, a slight shift in peak positions of ±0.2° compared to that of the standard ZnO crystal (34.45°) was observed. The ionic radii of Zn^{2+} and Al^{3+} are 0.074 and 0.054 nm, respectively, so the lattice spacing (d) between the (002) planes was expected to decrease when Al^{3+} ions were substituted into Zn^{2+} sites in the films. However, the peak position not only depends on the substitution of Al^{3+} for Zn^{2+} but also is strongly related to other parameters, such as sputtering conditions and the presence of electric fields [20].

Surface morphology is one of the most important properties of AZO films with regard to electronic device applications. A rough surface will decrease carrier mobility, increase resistivity, and deteriorate the performance of electrical devices. The crystallinity and crystallite size of the AZO films depended on the substrate temperature and gas flow rate.

This decrease in the $I_{(002)/(103)}$ ratio may be a result of the improved stoichiometry of the films associated with the incorporation of oxygen at oxygen vacancies.

The electrical properties of AZO films were determined by using Hall-effect measurements. As shown in Figure 3, the carrier densities were 1.41×10^{20}, 1.69×10^{21}, 8.01×10^{18}, and 6.16×10^{17} cm^{-3}, for A450-7, A350-7, A350-14, and A350-21, respectively. The charge-carrier density increased as the deposition temperature increased from 350 to 450°C. In addition, the carrier density tended to decrease as the gas flow rate increased. The carrier concentration in the AZO films decreased with increasing oxygen content produced by the changes in substrate temperature and oxygen gas flow rate; that is, O^{2-} ions could occupy the Zn^{2+} sites and play the role of electron acceptors, which caused a decrease in carrier density. The Hall mobility values were 0.59, 2.59, 12.59, and 29.06 $cm^2\ V^{-1}\ s^{-1}$ for S450-7, A350-7, A350-14, and A350-21, respectively. The mobility slightly increased as the substrate temperature decreased and the oxygen gas flow rate increased. These results corresponded with those reported by Lee et al. [21].

It was inferred that the electrical properties are affected by surface structure of the thin films. As shown in Figure 2, the c-axis was oriented perpendicularly to the substrate surface, and with decreasing gas flow rate the ordered crystallinities increased significantly. Moreover, the carrier density decreased rapidly, and the electrical resistance of the thin film increased, due to the distribution of the numerous ZnO grains that did not possess a stoichiometric composition. This interpretation was supported by the decrease in the $I_{(002)/(103)}$ peak-intensity ratio with increasing oxygen gas flow, as shown in Figure 2.

Figure 4 shows the XPS O1s spectra of the AZO films. Zn2p spectra were similar for all groups, and Al spectra were not detected due to low concentration of Al in AZO films. The O1s spectra are composed of two distinct components positioned at around 530 and 532 eV. The component at the lower binding energy (the "A" peak) was attributed to the difference in the electronegativity of oxygen and zinc. Also, peak A was related to the O^{2-} ions surrounded by Zn atoms in the wurtzite structure. This peak is related to the stoichiometry of the thin films. The binding energy peak near 532 eV (the "B" peak) had two O1s components: one most likely related to O in the ZnO phase and the other to the adsorbed molecular oxygen from the atmosphere on the oxide thin films [22]. The B peak is usually attributed to the presence of loosely bound oxygen on the surface or

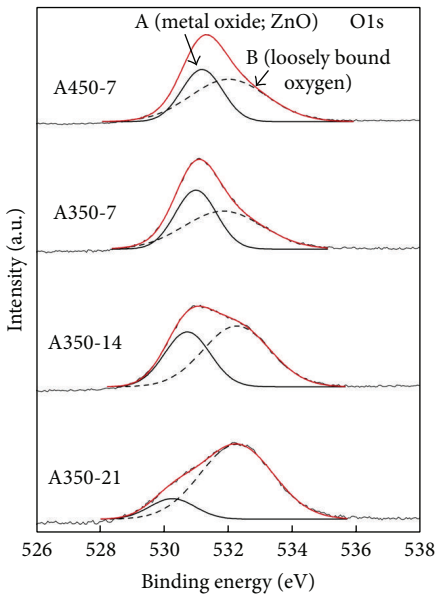

Figure 4: XPS O1s spectra of the AZO films.

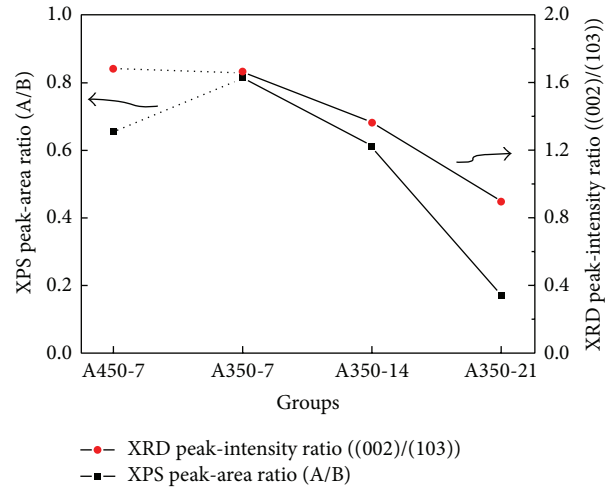

Figure 5: O1s XPS A/B peak-area ratios and the (002)/(103) XRD peak-intensity ratios.

hydrated oxide species such as adsorbed CO_3, H_2O, and O_2 [23–25]. Clearly, there are a significant number of absorbed oxygen ions on the surface of the ZnO thin films. It was inferred that the results of XPS were clearly related to the stoichiometry of AZO film. The higher area of peak B showed the lower stoichiometric properties of AZO film. So, A350-21 group had the numerous ZnO grains that did not possess a stoichiometric composition.

These results are in agreement with those obtained from the Hall carrier density measurement. As shown Figure 3, the charge-carrier concentrations of the films decreased gradually as the gas flow rate concentration increased, and the carrier density tended to decrease as the deposition temperature increased.

Figure 5 shows the area ratios of the A and B O1s XPS peaks (A/B) and the peak-intensity ratios of the (002) and (103) XRD peaks. The value of the A/B ratio decreased as the stoichiometric composition changed with increasing temperature and gas flow rate. The trend in the $I_{(002)/(103)}$ peak ratio with gas flow rate was similar to that of the A/B ratio. This result indicated that the crystalline structure of the ZnO film was closely connected to its stoichiometric composition. Also, as shown in Figure 3, the change in carrier density coincided with the change in the XPS peak-area ratio. We expected that the electron concentration at the lower deposition temperature would be lower because the formation of defects like oxygen or zinc vacancies requires some activation energy. With defect concentration increase, the carrier density increased and the resistivity decreased.

However, as the substrate temperature increased, the crystal growth direction of the surface became disordered and more surface area was exposed to air. Moreover, the carrier density decreased rapidly and the electric resistance of the thin film increased due to the distribution of many ZnO grains that did not satisfy the stoichiometric composition.

4. Conclusions

In conclusion, using a ceramic ZnO target, we produced transparent and conductive AZO thin films on a Si substrate using RF magnetron sputtering. With increasing substrate temperature and decreasing gas flow rate during deposition, the *c*-axis was increasingly oriented perpendicularly to the substrate surface. Moreover, the carrier density concentration increased rapidly and the electrical resistance of the thin film decreased due to the development of numerous ZnO grains without the stoichiometric composition.

Conflict of Interests

The authors declare that there is no conflict of interests regarding the publication of this paper.

Acknowledgment

This work was supported by research fund from Chosun University, 2014.

References

[1] B. Lin, Z. Fu, and Y. Jia, "Green luminescent center in undoped zinc oxide films deposited on silicon substrates," *Applied Physics Letters*, vol. 79, no. 7, article 943, 2001.

[2] A. Suzuki, T. Matsushita, N. Wada, Y. Sakamoto, and M. Okuda, "Transparent conducting Al-doped ZnO thin films prepared by pulsed laser deposition," *Japanese Journal of Applied Physics*, vol. 35, pp. L56–L59, 1996.

[3] D.-K. Hwang, H.-S. Kim, J.-H. Lim et al., "Study of the photoluminescence of phosphorus-doped *p*-type ZnO thin films grown by radio-frequency magnetron sputtering," *Applied Physics Letters*, vol. 86, no. 15, Article ID 151917, 2005.

[4] S. T. Shishiyanu, O. I. Lupan, E. V. Monaico, V. V. Ursaki, T. S. Shishiyanu, and I. M. Tiginyanu, "Photoluminescence of

chemical bath deposited ZnO:Al films treated by rapid thermal annealing," *Thin Solid Films*, vol. 488, no. 1-2, pp. 15–19, 2005.

[5] V. Srikant and D. R. Clarke, "Optical absorption edge of ZnO thin films: the effect of substrate," *Journal of Applied Physics*, vol. 81, no. 9, pp. 6357–6364, 1997.

[6] Z. Li and W. Gao, "ZnO thin films with DC and RF reactive sputtering," *Materals Letters*, vol. 58, no. 7-8, pp. 1363–1370, 2004.

[7] X.-T. Hao, L.-W. Tan, K.-S. Ong, and F. Zhu, "High-performance low-temperature transparent conducting aluminum-doped ZnO thin films and applications," *Journal of Crystal Growth*, vol. 287, no. 1, pp. 44–47, 2006.

[8] J. H. Jo, T.-B. Hur, J. S. Kwak, D. Y. Kwon, Y.-H. Hwang, and H. K. Kim, "Effects of oxygen pressure on the crystalline of ZnO films grown on sapphire by PLD method," *Journal of the Korean Physical Society*, vol. 47, article 300, 2005.

[9] Y. Natsume, H. Sakata, T. Hirayama, and H. Yanagida, "Low-temperature conductivity of ZnO films prepared by chemical vapor deposition," *Journal of Applied Physics*, vol. 72, no. 9, pp. 4203–4207, 1992.

[10] H. Mondragon-Suarez, A. Maldonaldo, M. de la et al., "ZnO:Al thin films obtained by chemical spray: effect of the Al concentration," *Applied Surface Science*, vol. 193, no. 1–4, pp. 52–59, 2002.

[11] B. J. Jin, H. S. Woo, S. Im, S. H. Bae, and S. Y. Lee, "Relationship between photoluminescence and electrical properties of ZnO thin fillms grown by pulsed laser deposition," *Applied Surface Science*, vol. 521, pp. 169–170, 2001.

[12] X. Q. Meng, W. Zhen, J. P. Guo, and X. J. Fan, "Structural, optical and electrical properties of ZnO and ZnO-Al_2O_3 films prepared by dc magnetron sputtering," *Applied Physics A*, vol. 70, no. 4, pp. 421–424, 2000.

[13] T. Minemoto, T. Negami, S. Nishiwaki, H. Takakura, and Y. Hamakawa, "Preparation of $Zn_{1-x}Mg_xO$ films by radio frequency magnetron sputtering," *Thin Solid Films*, vol. 372, no. 1, pp. 173–176, 2000.

[14] T. Minami, H. Sonohara, T. Kakumu, and S. Takata, "Highly transparent and conductive $Zn_2In_2O_5$ thin films prepared by RF magnetron sputtering," *Japanese Journal of Applied Physics*, vol. 34, no. 8, part 2, p. L971, 1995.

[15] T. Minami, T. Yamamoto, and T. Miyata, "Highly transparent and conductive rare earth-doped ZnO thin films prepared by magnetron sputtering," *Thin Solid Films*, vol. 366, no. 1-2, pp. 63–68, 2000.

[16] K. Tominaga, M. Kataoka, H. Manabe, T. Ueda, and I. Mori, "Transparent ZnO:Al films prepared by co-sputtering of ZnO:Al with either a Zn or an Al target," *Thin Solid Films*, vol. 290-291, pp. 84–87, 1996.

[17] G. K. Paul, S. Bandyopadhyay, S. K. Sen, and S. Sen, "Structural, optical and electrical studies on sol–gel deposited Zr doped ZnO films," *Materials Chemistry and Physics*, vol. 79, no. 1, pp. 71–75, 2003.

[18] J. Jeong and S. P. Choi, "A study of oxygen vacancy on SnO_2 thin films," *Journal of the Korean Institute of Electrical and Electronic Material Engineers*, vol. 18, no. 2, pp. 109–115, 2005.

[19] K. C. Park, D. Y. Ma, and K. H. Kim, "The physical properties of Al-doped zinc oxide films prepared by RF magnetron sputtering," *Thin Solid Films*, vol. 305, no. 1-2, pp. 201–209, 1997.

[20] P. Nunes, D. Costa, E. Fortunato, and R. Martins, "Performances presented by zinc oxide thin films deposited by r.f. magnetron sputtering," *Vacuum*, vol. 64, no. 3-4, pp. 293–297, 2002.

[21] C. Lee, K. Kim, and K. Prabakar, "Characterization of ZnO: Al-thin-film-passivated porous silicon," *Journal of the Korean Physical Society*, vol. 48, no. 6, pp. 1193–1198, 2006.

[22] L. Colombin, A. Jelli, J. Riga, J. J. Pireaux, and J. Verbist, "Penetration depth of tin in float glass," *Journal of Non-Crystalline Solids*, vol. 24, no. 2, pp. 253–258, 1977.

[23] Y.-S. Kim, W.-P. Tai, and S.-J. Shu, "Effect of preheating temperature on structural and optical properties of ZnO thin films by sol-gel process," *Thin Solid Films*, vol. 491, no. 1-2, pp. 153–160, 2005.

[24] M. Chen, W. Wang, Y. H. Yu et al., "X-ray photoelectron spectroscopy and auger electron spectroscopy studies of Al-doped ZnO films," *Applied Surface Science*, vol. 158, no. 1-2, pp. 134–140, 2000.

[25] C. C. Yang, C. C. Lin, C. H. Peng, and S. Y. Chen, "Effect of annealing atmosphere on physical characteristics and photoluminescence properties of nitrogen-implanted ZnO thin films," *Journal of Crystal Growth*, vol. 285, no. 1-2, pp. 96–102, 2005.